Clays and Clay Minerals, Vol. 32, No. 5, 400–406, 1984.

COLLOID STABILITY OF CLAYS USING PHOTON CORRELATION SPECTROSCOPY

B. E. NOVICH AND T. A. RING

Department of Materials Science and Engineering, Massachusetts Institute of Technology
Cambridge, Massachusetts 02139

Abstract—Photon correlation spectroscopy (PCS), a dynamic light-scattering technique for particle size measurement, was used to determine the coagulation rates of aqueous dispersions of relatively monodisperse South Carolina Peerless kaolinite, Silver Hill, Montana, illite, Wyoming montmorillonite, and Florida palygorskite. This technique allows quantitative measurement of the rate of coagulation for clay particles where the traditional turbidity method gives only a qualitative measure. The critical coagulation concentrations for KCl at pH = 10.0 were: 0.199 M for kaolinite, 0.202 M for illite, 0.290 M for montmorillonite, and 0.034 M for palygorskite. The effective Hamaker constants, calculated using Derjaguin-Landau-Verwey-Overbeek theory, were: 3.1×10^{-20} J for kaolinite, 2.5×10^{-20} J for illite, 2.2×10^{-20} J for montmorillonite, and 1.63×10^{-19} J for palygorskite. Stern potentials at the critical coagulation concentration at pH 10.0 were: −42.7 mV for kaolinite, −40.7 mV for illite, −21.2 mV for montmorillonite, and −66.9 mV for palygorskite.

Key Words—Coagulation rate, Hamaker constant, Illite, Kaolinite, Light scattering, Montmorillonite, Palygorskite, Photon correlation spectroscopy, Stern potential.

INTRODUCTION

The colloidal stability of aqueous dispersions of clay particles is critical to the design of clay processing operations (e.g., filtration, sedimentation, and ceramic processing). Recently, Novich (1983) related clay colloid stability to the geotechnical properties of waste clay tailings and showed a parallel relationship between slurry yield strength and the engineering properties of the slurry and soil. Coagulation rates for colloids have been measured in the past 50 years by direct methods, such as direct counting in the ultramicroscope (Overbeek, 1952) or in the Coulter counter (Mathews and Rhodes, 1970) in which sample disturbance and aging give highly variable results, and by indirect methods such as total-intensity light scattering (Lips and Willis, 1973; Bleier and Matijević, 1976; Sasaki *et al.*, 1980) and turbidimetry (Reerink and Overbeek, 1954; Weise and Healy, 1975), in which particle morphology and size have strong effects.

Photon correlation spectroscopy (PCS) is a dynamic light-scattering technique which directly measures particle size from fluctuations in scattered intensity occurring over very short time intervals due to Brownian motion of the colloidal particles in suspension (Cummings and Pusey, 1977; Chu, 1974). PCS is particularly suited for monitoring clay coagulation because it measures the hydrodynamic particle size independent of particle shape (Barringer *et al.*, 1983). The several associative processes that occur during coagulation can be generalized as the interaction of an m-particle aggregate with an n-particle aggregate to form an (n + m)-particle aggregate. During the initial stage of coagulation, the formation of doublets from singlets dominates the process. Detailed theoretical predictions for doublet formation are available which consider Brownian motion (von Smoluchowski, 1917), interparticle forces (Tambour and Sienfeld, 1980; Marmur, 1979), and hydrodynamic interactions (Spielman, 1970; Honig *et al.*, 1971). The present study employed photon correlation spectroscopy to measure the rate of doublet formation in coagulating suspensions. The measurement of this rate at various salt concentrations allowed critical coagulation concentration (CCC) to be determined for the clay-electrolyte system. PCS experiments were performed using narrow size ranges of kaolinite, illite, montmorillonite, and palygorskite as a function of KCl ionic strenth at pH = 10.0.

According to Derjaguin-Landau-Verwey-Overbeek theory, clay colloid stability (i.e., whether or not the clay will coagulate and the magnitude of energy associated with the coagulation process), is a function of several particle and solution properties. The total interaction energy, V_T, is given by (van Olphen, 1977):

$$V_T = V_A + V_R, \quad (1)$$

where

$$V_A = \frac{A_{121}}{48\pi}[d^{-2} + (d + \Delta)^{-2} - 2(d + \Delta/2)^{-2}], \quad (2)$$

where A_{121} is the effective Hamaker constant for a clay (phase 1)-water (phase 2)-clay (phase 1) interaction, d is the half distance between the coagulating particles, and Δ is the particle thickness. For flat plates like montmorillonite (Δ = 6.6 Å), d is similar to Δ. For block-like particles (e.g., kaolinite, illite, and palygorskite), d is much less than Δ, and Eq. (2) may be rewritten

$$V_A = A_{121}/(48\pi d^2). \quad (3)$$

V_R is the double layer repulsive energy:

$$V_R = (64nkT/\kappa)\gamma^2\exp(-2\kappa d), \quad (4)$$

where κ is the Debye-Hückel parameter, n is the ion concentration, k is Boltzmann's constant, T is the absolute temperature, and γ^2 is a double layer parameter that is dependent on the Stern potential. Using the cation-exchange capacity and specific surface area to calculate σ_0, the constant surface charge density and then γ^2, the total interaction energy (Eq.(1)) for aqueous systems, reduces to one equation and two unknowns, A_{121} and d.

The CCC corresponds to a point on the total interaction energy defined by $V_T = 0$ and $\delta V_T/\delta d = 0$. Applying these conditions to Eq. (1), two dependent equations result from which A_{121} and d can be calculated. The derivation of this approach is shown in Appendix 1. This derivation tacitly assumes that doublet formation is exclusively by face-to-face association and not by edge-to-face or edge-to-edge association. This assumption is reasonable, because at pH 10 both the edges and the faces are negatively charged and the probability of face-to-face association is higher than that of any other type of association.

The time dependence of the fluctuations in scattered light intensity in PCS is quantitatively described by the intensity autocorrelation function, $C(\tau)$:

$$C(\tau) = \langle I^*(K,t)I(K,t+\tau)\rangle, \quad (5)$$

where I is the scattered intensity, t is the time, τ is the delay time, and K is the magnitude of the scattering vector, defined as

$$K = (4\pi n/\lambda_0)\sin(\theta/2), \quad (6)$$

where n is the refractive index of the medium, θ is the scattering angle, and λ_0 is the incident wavelength of the light measured in vacuum.

In the Gaussian approximation, the intensity autocorrelation function is related to the field autocorrelation function, $g'(\tau)$, by

$$C(\tau) = 1 + |g'(\tau)|^2, \quad (7)$$

where

$$g'(\tau) = \langle E^*_s(K,t)E_s(K,t+\tau)\rangle, \quad (8)$$

and E_s is the scattered electric field. For a suspension of monodisperse, spherical particles, $g'(\tau)$ is given by

$$g'(\tau) = \exp(-\Gamma\tau), \quad (9)$$

where $\Gamma = DK^2$. The translational, z-averaged diffusion coefficient of the particle, D, is related to the hydrodynamic radius, R_h, by the Stokes-Einstein equation:

$$D = kT/6\pi\eta R_h, \quad (10)$$

where k is Boltzmann's constant, T is the absolute temperature, and η is the viscosity of the medium.

Polydisperse systems can be analyzed by replacing Eq. (9) with

$$g'(\tau) = \int_0^\infty G(\Gamma)\exp(-\Gamma\tau)\,d\Gamma \quad (11)$$

and

$$\int_0^\infty G(\Gamma)\,d\Gamma = 1, \quad (12)$$

where $G(\Gamma)$ is the normalized distribution function in Γ space. Thus, the autocorrelation function theoretically contains complete information about the particle size distribution.

One technique of analyzing PCS data is the method of cumulants (Koppel, 1972), which expands the right-hand side of Eq. (11) in a Taylor series about the mean, $\bar{\Gamma}$:

$$\ln|g'(\tau)| = -\bar{\Gamma}\tau + (1/2!)\mu_2\tau^2 - (1/3!)\mu_3\tau^3 + \ldots \quad (13)$$

The cumulants (μ_2, μ_3, . . .) are related to the moments of the particle size distribution; however, in practice only the first and second cumulants ($\bar{\Gamma}$ and μ_2) can be reliably obtained. The ratio $\mu_2/\bar{\Gamma}^2$ is the variance of the distribution function $G(\Gamma)$ and is a measure of the polydispersity of the suspension.

In the coagulation experiments, $\bar{\Gamma}$ and $\mu_2/\bar{\Gamma}^2$ are obtained as a function of time; the value of $\bar{\Gamma}$ is converted to a mean hydrodynamic radius, $\bar{R}_h$, using Eq. (10). During the early stage of coagulation, the mean hydrodynamic radius is dependent on the fraction of doublets, X, and the fraction of singlets, (1 − X):

$$\bar{R}_h = (1 - X)R_{h,1} + XR_{h,2}, \quad (14)$$

where $R_{h,1}$ and $R_{h,2}$ are the radii of the singlet and the doublet, respectively. The hydrodynamic radius of the doublet can be approximated by the surface diameter of the doublet for low Reynolds numbers (Allen, 1981). Thus,

$$R_{h,2} = \sqrt{2}\,R_{h,1}. \quad (15)$$

Substituting for $R_{h,2}$ in Eq. (10), the mean size becomes

$$\bar{R}_h = R_{h,1}[1 + X(\sqrt{2} - 1)]. \quad (16)$$

As coagulation proceeds and doublets form, the mean hydrodynamic radius increases; the time rate of increase is given by

$$d\bar{R}_h/dt = R_{h,1}(\sqrt{2} - 1)\,dX/dt. \quad (17)$$

The coagulation of singlets to form doublets obeys the following second-order rate law:

$$-dN/dt = k_S N^2, \quad (18)$$

https://doi.org/10.1346/CCMN.1984.0320508 Published online by Cambridge University Press

Table 1. Sample descriptions.

Sample	Origin	$\overline{PS}$ (μm)[1]	σ_A (μm)[2]
Kaolinite	South Carolina[3]	0.37	0.06
Illite	Silver Hill, Montana[4]	0.39	0.14
Montmorillonite	Crook County, Wyoming[5]	0.54	0.12
Palygorskite	Gadsden County, Florida[6]	0.47	0.15

[1] $\overline{PS}$ = mean particle size after size fractionation measured by photon correlation spectroscopy, pH = 10.1 (KOH), no KCl salt.

[2] σ_A = arithmetic standard deviation for the particle size distribution after size fractionation from photon correlation spectroscopy.

[3] Dixie Clay Company, Bath, South Carolina.

[4] The Clay Minerals Society, Source Clay Repository (IMt-1).

[5] The Clay Minerals Society, Source Clay Repository (SWy-1).

[6] The Clay Minerals Society, Source Clay Repository (PFl-1).

where k_S is the rate constant, N is the concentration of singlets given by

$$N = N_0(1 - X), \tag{19}$$

and N_0 is the initial concentration of singlets. Substituting Eq. (19) into Eq. (18) gives

$$dX/dt = k_S N_0(1 - X)^2. \tag{20}$$

At the initial stage of coagulation, the fraction of doublets is small, thus giving the approximation

$$\left.\frac{dX}{dt}\right|_{t\to 0} = k_S N_0. \tag{21}$$

By substituting Eq. (21) into Eq. (17) and solving for the rate constant, one obtains

$$k_S = [R_{h,1}(\sqrt{2} - 1)N_0]^{-1} \left.\frac{d\bar{R}_h}{dt}\right|_{t\to 0}. \tag{22}$$

Eq. (22) is only valid for the initial stage of coagulation, when the fraction of doublets is small. This was the case for the PCS coagulation experiments.

EXPERIMENTAL

Chemicals and glassware

All chemicals were analytical reagent grade and were used without further purification. The solutions were made using deionized water ($\rho > 17 \times 10^6$ ohm-cm). Solutions were prepared in volumetric flasks and stored in polypropylene bottles that had been thoroughly cleaned by acid (1 M HNO_3) and base (1 M KOH) washes. Solutions were filtered through 0.22-μm Millipore filters prior to the coagulation experiments. All experiments were performed at 25 ± 0.1°C.

Sample preparation

Coagulation experiments were carried out using four natural clay minerals: kaolinite, illite, montmorillonite, and palygorskite. Table 1 lists their sources and particle sizes after fractionation. Each clay, as received, was washed with deionized water and fractionated as follows: A 1% solids suspension at pH = 9.0 (KOH) was allowed to settle in a 6-liter cylindrical container for 15 hr at 25°C, so that all particles >1 μm had settled below the 5-cm level. The top 5 cm of the suspension was removed using a U-tube pipette and redispersed in a clean container. The <1-μm fractionation was repeated twice, followed by three successive fractionations to remove all particles >0.5 μm; the required sedimentation time was 59.3 hr at 25°C.

The particle concentration of each stock solution was determined by dry weight analysis using a density of 2.61 g/cm³ for kaolinite, 2.81 g/cm³ for illite, 2.74 g/cm³ for montmorillonite, and 2.09 g/cm³ for palygorskite (Lambe and Whitman, 1968).

Coagulation

The Malvern K7025 correlator (Malvern Ltd.) used in this study was similar to those described in the literature (Cummings and Pusey, 1977; Yates, 1975; Weise and Healy, 1975). The light source was the 632.8-nm line of a Spectra Physics 35 mW He-Ne laser. The scattered intensity was measured at a fixed angle of 90° by an ITT FW 130 photomultiplier tube. The 120-channel correlator was controlled by a Commodore 3032 computer, which also analyzed the correlation functions to yield D, the average effective diffusion coefficient, and $\bar{R}_h$, the average hydrodynamic radius for the particles in suspension. Optimal operating parameters for the correlator were a 200-μsec sample time and 2×10^5 samples, which allowed data to be taken and analyzed at a rate of one average hydrodynamic radius per minute using the complete cumulant analysis method (Cummings and Pusey, 1977; Koppel, 1972). Selection of the parameters for coagulation experiments required a compromise between accuracy and sampling (+ analysis) speed. Speed was especially critical for unstable systems; data for a size measurement was obtained rapidly enough so that the change in average particle size during a measurement was always less than 10% of the previous value.

A specific coagulation experiment was performed by diluting a stock suspension into a solution having the desired KCl salt concentration, contained in a 3-ml glass cuvette so that the final clay concentration was approximately 10^8 particles/cm³ (0.01 wt. %). The pH was adjusted to 10.0 immediately prior to stock addition. The cuvette was capped, quickly inverted several times to mix the contents, and then transferred to the correlator for analysis. The time between stock addition and analysis initiation was typically <10 sec.

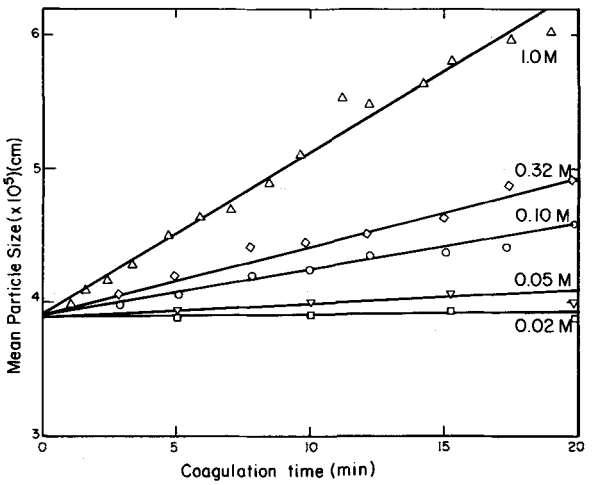

Figure 1. Mean particle size vs. coagulation time for illite in various KCl solutions at pH 10.0. $N_0 = 1.57 \times 10^8$ particles/cm³.

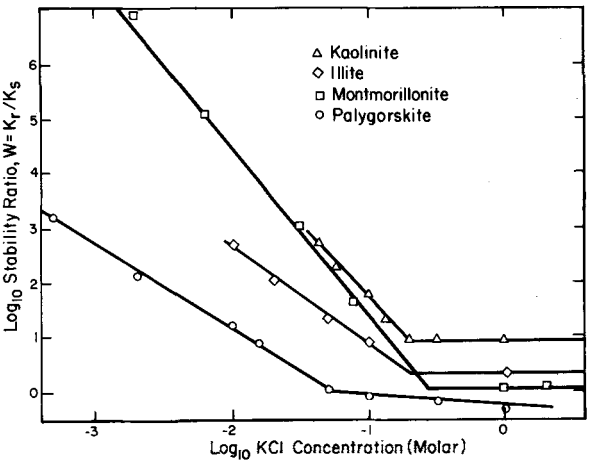

Figure 2. Stability ratio vs. KCl concentration for kaolinite, illite, montmorillonite, and palygorskite at pH 10.0.

Sample pH was assessed by measuring the pH of an identical sample immediately after preparation and of the coagulated sample upon completion of the coagulation experiment; data were discarded for pH deviations >0.2 units.

An example of the coagulation data taken for illite is given in Figure 1. Here the mean particle size is plotted as a function of coagulation time. The coefficients of determination (r^2) for these lines ranged between .89 and .92 for a minimum of 10 data points. The highest slope was observed with 1.0 M KCl, the lowest with 0.02 M KCl. The average slope, $d\bar{R}_h/dt$, was used to calculate the coagulation rate constant, K_S, from Eq. (22) and the stability ratio, W,

$$W = k_R/k_S, \quad (23)$$

where k_R is the rapid coagulation rate constant defined by von Smoluchowski (1917) as

$$k_R = 8kT/(3\eta), \quad (24)$$

where k is Boltzmann's constant, T is the absolute temperature, and η is the viscosity of the fluid medium.

RESULTS AND DISCUSSION

Critical coagulation concentration

The KCl stability curves for the four types of clay at pH = 10.0 are shown in Figure 2. The CCC is the concentration corresponding to the intersection of the slow and rapid coagulation curves. The CCCs for KCl at pH = 10.0 were: 0.199 M for kaolinite, 0.202 M for illite, 0.290 M for montmorillonite, and 0.034 M for palygorskite. The CCCs for the platelet clays, kaolinite, illite, and montmorillonite, were roughly the same. The CCC for palygorskite was approximately 1/10 less, indicating a greater tendency toward coagulation. The difference is attributed to the fibrous morphology of palygorskite, which increases the surface-to-volume ratio of the particles, causing an increase in coagulation rate for a given salt concentration. The four CCCs are within the range of CCCs given by van Olphen (1977) for monovalent salt in clay coagulation.

Effective Hamaker constant

The effective Hamaker constant, A_{121}, was calculated for each clay from experimentally determined CCCs using an augmented Reerink and Overbeek (1954) analysis which employed the parallel plate form of the interaction energies. This approach is derived in Appendix 1. The derivation uses values of specific surface area and the cation-exchange capacity. Both are given in Table 2 for each clay. The effective Hamaker constant, A_{121}, and the Stern potential, ψ_δ, at the CCC were calculated using this derivation. These values are given in Table 3.

The effective Hamaker constant, A_{121}, for illite measured in this study, 2.50×10^{-20} J, was within experimental error of the A_{121} value, $2.2 \pm 0.3 \times 10^{-20}$ J, obtained by Israelachvilli and Adams (1978) for mica plates in an aqueous solution of KNO_3. The value ob-

Table 2. Typical values of cation-exchange capacity (CEC) and specific surface area (SSA) used in A_{121} calculation.

Clay	CEC (meg/100 g)[1]	SSA (m^2/g)[1]	σ_0 (esu/cm²)[2]
Kaolinite	2	10	5.8×10^4
Illite	27	89	8.7×10^4
Montmorillonite	76	662	3.4×10^4
Palygorskite	20	136	4.2×10^4

[1] Van Olphen and Fripiat (1979).
[2] Calculated values from CEC and SSA.

https://doi.org/10.1346/CCMN.1984.0320508 Published online by Cambridge University Press

Table 3. Effective Hamaker constants (A_{121}), Hamaker constants (A_{11}), and Stern potentials (ψ_δ).

Clay	$A_{121} \times 10^{20}$ (J)[1]	$A_{11} \times 10^{19}$ J[2]	ψ_δ (CCC) (mV)
Kaolinite	3.1	1.5	−42.7
Illite	2.5	1.4	−40.7
Montmorillonite	2.2	1.3	−21.2
Palygorskite	16.3	3.8	−66.9

[1] Experimental; 1-2-1: clay-water-clay.
[2] Calculated from A_{121} and A_{22} (water-water) = 4.4×10^{-20} J (Krupp *et al.*, 1972), using geometric mixing rule.

tained in this study is equal to A_{121} calculated using the geometric mixing rule, and $A_{11} = 1.3 \times 10^{-19}$ J determined by Tabor and Winterton (1969) for mica plates in a vacuum and $A_{22} = 4.38 \times 10^{-20}$ J determined by Krupp *et al.* (1972) for water. No data relative to the Hamaker constants for kaolinite, montmorillonite, or palygorskite have been reported in the literature. The values of A_{121} measured for kaolinite, 3.1×10^{-20} J, and for montmorillonite, 2.2×10^{-20} J, are consistent with the A_{121} measured for illite, 2.5×10^{-20} J; all three clays have similar crystal chemistry and particle morphology. The relatively high value of A_{121} for palygorskite, 16.3×10^{-20} J, calculated using a parallel plate analysis, is consistent with relatively strong coagulation observed in sedimentation experiments by Novich (1983). This parallel plate analysis for palygorskite may be slightly inaccurate, inasmuch as palygorskite is a fiber and not a flat plate. Values of A_{11} (clay-clay) given in Table 3 were calculated using the geometric mixing rule and a value of A_{22} for water of 4.38×10^{-20} J (Krupp *et al.*, 1972).

Stern potentials

The Stern potential, ψ_δ, can be calculated from

$$\psi_\delta = Z_\delta kT/\nu e, \qquad (25)$$

where ν is the valence of the counter ions, e is the fundamental charge, and Z_δ is the reduced Stern potential given by Eq. (A-9). The Stern potential at the CCC for each of the clay minerals is given in Table 3. The Stern potential for kaolinite, −42.7 mV, is very close to the zeta potential of −41.1 mV measured by Williams and Williams (1978) for kaolinite at 10^{-2} M NaCl and pH = 10.0. The Stern potential for montmorillonite, −21.2 mV, is similar to the zeta potentials for Ca-bentonite (−33.4 mV) and for Na-bentonite (−43.6 mV) measured by van Olphen (1957). Van Olphen gave no information about suspension pH or salt concentration, which affect the zeta potential. Friend and Hunter (1970) found the zeta potential of Na-bentonite to be independent of 1:1 electrolyte concentration and reported a zeta potential of −30 mV at 0.1 M NaCl. May and Smelley (1979) measured a zeta potential of −46 mV for palygorskite at pH = 10.0 at an unspecified salt concentration. This value is considerably lower than the Stern potential calculated for palygorskite in the present study (−66.9 mV). Zeta potential data for illite are not available in the literature.

CONCLUSIONS

Photon correlation spectroscopy has been successfully used to measure the coagulation rate of fractionated kaolinite, illite, montmorillonite, and palygorskite in KCl solutions at pH = 10.0. This technique determined the critical coagulation concentration at pH 10.0 for each clay tested: kaolinite = 0.199 M; illite = 0.202 M; montmorillonite = 0.290 M; and palygorskite = 0.034 M KCl. The CCCs were used in the D.L.V.O. theory of colloid stability to determine the effective Hamaker constants: kaolinite = 3.1×10^{-20} J; illite = 2.5×10^{-20} J; montmorillonite = 2.2×10^{-20} J; and palygorskite = 16.3×10^{-20} J; and Stern potentials: kaolinite = −42.7 mV; illite = −40.7 mV; montmorillonite = −21.2 mV; and palygorskite = −66.9 mV at the CCC. These results compared favorably to literature values and complementary studies.

ACKNOWLEDGMENT

The authors thank Dr. R. Torrence Martin for his critical review of this manuscript.

APPENDIX I

The calculation of the effective Hamaker constant, A_{121}, for the clay minerals is based on the method of Reerink and Overbeek (1954). Using Derjaguin-Landau-Verwey-Overbeek theory, two curves are derived from the total interaction energy, the intersection of which corresponds to the critical coagulation state. At the critical coagulation concentration,

$$V_T = 0 \qquad (A\text{-}1)$$

and

$$\partial V_T/\partial d = 0, \qquad (A\text{-}2)$$

where d is the half distance between two coagulating particles and V_T is the total interaction energy,

$$V_T = V_A + V_R \qquad (A\text{-}3)$$

which is equal to the sum of the Van der Waals attractive energy, V_A, and the double layer repulsive energy, V_R.

For montmorillonite the particle thickness, Δ, is on the order of d,

$$V_A = \frac{-A_{121}}{48\pi}(d^{-2} + (d + \Delta/2)^{-2}), \qquad (A\text{-}4)$$

where Δ = 6.6 Å for montmorillonite (van Olphen, 1977). For other clays where $\Delta \gg d$,

$$V_A = -A_{121}/(48\pi d^2). \qquad (A\text{-}5)$$

The double layer repulsive energy is given by

$$V_R = (64nkT/\kappa)\gamma^2\exp(-2\kappa d), \qquad (A\text{-}6)$$

where n is the ion concentration, k is Boltzmann's constant, T is the absolute temperature, κ is the Debye-Hückel parameter given by

$$\kappa = 3.29 \times 10^7 |\nu| M^{1/2} (cm^{-1}) \qquad (A\text{-}7)$$

at 25°C for a symmetrical electrolyte, where ν is the valence of the cation and M is the molar concentration.

γ^2 is defined as

$$\gamma^2 = [(e^{Z_\delta/2} - 1)/(e^{Z_\delta/2} + 1)]^2, \qquad (A\text{-}8)$$

where Z_δ is the reduced Stern potential given by van Olphen (1977) as

$$Z_\delta = \ln\left[\left(\frac{\sigma_0}{\beta(2\cosh Z_\delta - 2)^{1/2}} - 1\right)\cdot\left(\frac{d-\delta}{\delta}\right)\right], \qquad (A\text{-}9)$$

where σ_0 is the constant surface charge density, δ is the thickness of the Stern layer (~3 Å), and

$$\beta = (\epsilon nkT/2\pi)^{1/2}, \qquad (A\text{-}10)$$

where ϵ is the dielectric constant for the fluid. σ_0 can be calculated from the cation-exchange capacity and the specific surface area.

Applying Eqs. (A-1) and (A-2) to Eq. (A-3) and solving the resulting two equations simultaneously at the CCC gives:

$$\kappa_c = \frac{d_c^{-3} + (d_c + \Delta)^{-3} - 2(d_c + \Delta/2)^{-3}}{d_c^{-2} + (d_c + \Delta)^{-2} - 2(d_c + \Delta/2)^{-2}} \qquad (A\text{-}11)$$

for montmorillonite and

$$\kappa_c d_c = 1 \qquad (A\text{-}12)$$

for kaolinite, illite, and palygorskite.

Solving Eqs. (A-11) or (A-12) for d_c, Eq. (A-1) or (A-2) can be solved for A_{121}. For example, Eq. (A-2) is

$$A_{121} = \frac{9651\ nkT\gamma^2\exp(-2\kappa_c d_c)}{d_c^{-3} + (d_c + \Delta)^{-3} - 2(d_c + \Delta/2)^{-3}} \qquad (A\text{-}13)$$

for montmorillonite and

$$A_{121} = 1306nkT\gamma^2 d_c^3 \qquad (A\text{-}14)$$

for kaolinite, illite, and palygorskite.

REFERENCES

Allen, T. (1981) *Particle Size Measurement:* 3rd ed., Chapman and Hall Publ., London, 104 pp.

Barringer, E. A., Novich, B. E., and Ring, T. A. (1983) Colloidal stability of ceramic powders using photon correlation spectroscopy: *J. Colloid Interface Sci.* (in press).

Bleier, A. and Matijević, E. (1976) Heterocoagulation. VI. Interactions of a monodispersed chromium hydroxide with polyvinyl chloride latex: *J. Colloid Interface Sci.* **55,** 510–535.

Chu, B. (1974) *Laser Light Scattering:* Academic Press, N.Y., 318 pp.

Cummings, H. Z. and Pusey, P. N. (1977) Dynamics of macromolecular motion: in *Photon Correlation Spectroscopy and Velocimetry,* H. Z. Cummings and E. R. Pike, eds., Plenum Press, N.Y., 164–199.

Friend, J. P. and Hunter, R. J. (1970) Vermiculite as a model system in the testing of double layer theory: *Clays & Clay Minerals* **18,** 275–283.

Honig, E. P., Roberson, G. J., and Wiersema, P. H. (1971) Effect of hydrodynamic interaction on the coagulation rate of hydrophobic colloids: *J. Colloid Interface Sci.* **36,** 97–109.

Israelachvilli, J. N. and Adams, G. E. (1978) Measurement of forces between two mica surfaces in aqueous electrolyte solutions in the range 0–100 nm: *J. Chem. Soc., Faraday Trans. I* **74,** 975–1001.

Koppel, D. E. (1972) Analysis of macromolecular polydispersity in intensity correlation spectroscopy: the method of cumulants: *J. Chem. Phys.* **57,** 4814–4820.

Krupp, H., Schnabel, W., and Walter, G. (1972) The Lifshitz-Van der Waals constant on the basis of optical data: *J. Colloid Interface Sci.* **39,** 421–423.

Lambe, T. W. and Whitman, R. V. (1968) *Soil Mechanics:* Wiley, N.Y., 29–40.

Lips, A. and Willis. E. (1973) Low angle light scattering technique for the study of coagulation: *J. Chem. Soc., Faraday Trans. I* **69,** 1226–1236.

Marmur, A. (1979) A kinetic theory approach to primary and secondary minimum coagulations and their combination: *J. Colloid Interface Sci.* **72,** 41–48.

Mathews, B. A. and Rhodes, C. T. (1970) Studies of the coagulation kinetics of mixed suspensions: *J. Colloid Interface Sci.* **32,** 332–338.

May, A. and Smelley, A. G. (1979) Effects of electrolytes on the electrophoretic mobilities of Florida phosphatic clay wastes: *Bur. Mines Rept. Invest.* **RI 8398,** 1–13.

Novich, B. (1983) Composition and rheology of Florida phosphatic waste clay slurries: geotechnical implications: M.S. thesis, Dept. of Civil Engineering, Massachusetts Institute of Technology, Cambridge, Mass., 252 pp.

Overbeek, J. Th. G. (1952) Coagulation phenomena: in *Colloid Science, Vol. 1,* H. R. Kruyt, ed., Elsevier, London, p. 159.

Reerink, H. and Overbeek, J. Th. G. (1954) The rate of coagulation as a measure of the stability of silver iodide sols: *Disc. Faraday Soc.* **18,** 74–84.

Sasaki, H., Matejević, E., and Barouch, E. (1980) Heterocoagulation. VI. Interactions of a monodispersed hydrous aluminum oxide sol with polystyrene latex: *J. Colloid Interface Sci.* **76,** 319–329.

Spielman, L. (1970) Viscous interactions in Brownian coagulation: *J. Colloid Interface Sci.* **33,** 562–571.

Tabor, D. and Winterton, R. H. S. (1969) The direct measurement of normal and retarded Van der Waals forces: *Proc. Roy. Soc.* **A312,** 435–450.

Tambour, V. and Seinfeld, J. H. (1980) Solution of the discrete coagulation equation: *J. Colloid Interface Sci.* **74,** 260–272.

van Olphen, H. (1957) Surface conductance of various ion forms of bentonite in water and the electrical double layer: *J. Amer. Chem. Soc.* **61,** 1276–1280.

van Olphen, H. (1977) *Introduction to Clay Colloid Chemistry:* 2nd ed., Wiley, N.Y., 318 pp.

van Olphen, H. and Fripiat, J. J. (1979) *Data Handbook for*

Clay Materials and other Non-Metallic Minerals: Pergamon Press, New York, 346 pp.
von Smoluchowski, M. (1917) Versuch einer mathematischen Theorieder Koagulationskinetic kolloider Lösungen: *Z. Phys. Chem.* **92,** 129–168.
Weise, G. R. and Healy, T. W. (1975) Coagulation and electrokinetic behavior of TiO_2 and H_2O colloidal dispersions: *J. Colloid Interface Sci.* **51,** 427–433.
Williams, D. J. A. and Williams, K. P. (1978) Electrophoresis and zeta potential of kaolinite: *J. Colloid Interface Sci.* **65,** 79–87.
Yates, D. E. (1975) The structure of the oxide/aqueous electrolyte interface: Ph.D. thesis, University of Melbourne, Australia, 272 pp.

(Received 5 October 1983; accepted 9 March 1984)

Резюме—Фото-корреляцционная спектроскопия (ФКС), динамический, свет рассеивающий метод для измерений размера частиц, использовалась для определения скоростей коагуляции водных дисперсий относительно монодисперсионных каолинитов из Южной Каролины, иллита из Серебряного Холма, Монтана, монтмориллонита из Вайоминга и палыгорскита из Флориды. Этот метод позволяет измерять количественно скорость коагуляции частиц глины в случае, когда традиционный метод путем мутнения дает только качественное измерение. Критические концентрации коагуляции KCl при pH = 10 были: 0,199 M для каолинита, 0,202 M для иллита, 0,29 M для монтмориллонита, и 0,034 M для палыгорскита. Эффективные постоянные Гамакера, рассчитанные при использовании теории Держагина-Ландау-Веруэя-Овербика, составляли: $3{,}1 \times 10^{-20}$ дж для каолинита, $2{,}5 \times 10^{-20}$ дж для иллита, $2{,}2 \times 10^{-20}$ дж для монтмориллонита, и $1{,}63 \times 10^{-19}$ дж для палыгорскита. Потенциалы Штерна при критических концентрациях коагуляции при pH = 10,0 составляли: −42,7 мв для каолинита, −40,7 мв для иллита, −21,2 мв для монтмориллонита, и −66,9 мв для палыгорскита. [E.G.]

Resümee—Photonenkorrelationsspektroskopie (PCS), eine dynamische auf Lichtstreuung beruhende Technik zur Messung der Teilchengröße wurde verwendet, um die Koagulationsgeschwindigkeiten von wässrigen Dispersionen von relativ monodispersem South Carolina Peerless Kaolinit; Illit von Silver Hill, Montana; Montmorillonit von Wyoming; und Palygorskit von Florida zu bestimmen. Diese Methode erlaubt die quantitative Messung der Koagulationsgeschwindigkeit für Tonpartikel, während die herkömmliche Turbiditätsmethode nur qualitative Messungen ergibt. Die kritischen Koagulationskonzentrationen für KCl bei pH 10,0 waren: 0,199 m für Kaolinit; 0,202 m für Illit; 0,290 m für Montmorillonit; und 0,034 m für Palygorskit. Die wirksamen Hamaker-Konstanten, die unter Verwendung der Derjaguin-Landau-Verwey-Overbeek-Theorie berechnet wurden, waren: $3{,}1 \times 10^{-20}$ J für Kaolinit; $2{,}5 \times 10^{-20}$ J für Illit; $2{,}2 \times 10^{-20}$ J für Montmorillonit; und $1{,}63 \times 10^{-19}$ für Palygorskit. Die Stern-Potentiale bei der kritischen Koagulationskonzentration bei pH 10,0 waren −42,7 mV für Kaolinit; −40,7 mV für Illit; −21,2 mV für Montmorillonit; und − 66,9 mV für Palygorskit. [U.W.]

Résumé—La spectroscopie à corrélation de photons (PCS), une technique dynamique, éparpillant la lumière pour mesurer la taille de particules, a été utilisée pour déterminer les allures de coagulation des dispersions aqueuses relativement monodisperses de kaolinite Peerless de Caroline du Sud, d'illite de Silver Hill du Montana, de montmorillonite du Wyoming, et de palygorskite de Floride. Cette technique permet de mesurer l'allure de coagulation de particules d'argile de manière quantitative, tandis que la méthode traditionnelle de turbidité ne donne qu'une mesure qualitative. Les concentrations de coagulation critiques pour KCl au pH = 10,0 étaient: 0,199 M pour la kaolinite, 0,202 M pour l'illite, 0,290 M pour la montmorillonite, et 0,034 M pour la palygorskite. Les constantes éffectives d'Hamaker, calculées d'après la théorie Derjaguin-Landau-Verwey-Overbeek, étaient $3{,}1 \times 10^{-20}$ J pour la kaolinite, $2{,}5 \times 10^{-20}$ J pour l'illite, $2{,}2 \times 10^{-20}$ J pour la montmorillonite, et $1{,}63 \times 10^{-19}$ J pour la palygorskite. Les potentiels de Stern aux concentrations critiques de coagulation au pH 10,0 étaient: −42,7 mV pour la kaolinite, −40,7 mV pour l'illite, −21,2 mV pour la montmorillonite, et −66,9 mV pour la palygorskite. [D.J.]